

Green Synthesis and Characterization of Silver Nanoparticles Using *Ocimum Tenuiflorum* (Thulasi) Leaf Extract: Morphological Variations and Antibacterial Activity

Deepa S¹

Assistant professor, Department of Physics, Government College of Engineering, Salem.

deepasasi1984@gmail.com

Sasikumar P²

Professor, Department of Computer Science and Engineering, Malla Reddy Institute of Engineering and Technology

sasi.mca@gmail.com

Abstract

Silver nanoparticles (AgNPs) have garnered significant attention due to their unique electrical, optical, and biological properties, with applications spanning food, medicine, cosmetics, textiles, and water treatment. The growing demand for AgNPs necessitates environmentally friendly synthesis methods. This study focuses on the green synthesis of silver nanoparticles using *Ocimum tenuiflorum* (Thulasi) leaf extract as a reducing and stabilizing agent. The chemical constituents of Thulasi, such as oleanolic acid, ursolic acid, rosmarinic acid, and eugenol, contribute to its phytochemical properties, including antioxidant, antidiabetic, and anticancer activities. Thulasi extracts have been used to synthesize silver nanoflowers (AgNFs) and spherical silver nanoparticles under three deposition conditions: (1) mixing Thulasi extract with silver nitrate at ambient temperature, (2) stirring the mixture at elevated temperatures, and (3) prolonged blending of the extract and silver nitrate solution. The synthesized nanoparticles were characterized using scanning electron microscopy (SEM), energy dispersive X-ray spectroscopy (EDS), transmission electron microscopy (TEM), high-resolution TEM (HRTEM), selected area electron diffraction (SAED), and UV-Vis spectroscopy to analyze their structural and morphological variations. The study highlights the influence of synthesis conditions on nanoparticle shape, size, and properties, demonstrating the formation of AgNFs and spherical AgNPs. The antibacterial activity of the nanoparticles against pathogens like *Staphylococcus aureus* and *Escherichia coli* was further validated. These findings suggest that Thulasi-mediated AgNPs are promising for diverse applications, including antimicrobial agents in healthcare, food preservation, water purification, and beyond. This study underscores the significance of green synthesis in achieving sustainable and efficient nanoparticle production.

Keywords: Silver Nanoparticles, Green Synthesis, *Ocimum tenuiflorum* (Thulasi), Nanoparticle Morphology, Antibacterial Activity and Transmission Electron Microscopy.

1. INTRODUCTION

Nanoparticles of silver are essential to our day-to-day existence. They are highly electrically, optically, and biologically active. Because of their foligodynamic impact,

silver nanoparticles are employed as disinfectants. as the use of silver nanoparticles in food, drink, clothing, and medicine increases, so does the necessity for their manufacturing [1]. There are presently several physical and chemical methods available in the literature to synthesise silver nanoparticles;

however, the goal of this study is to create silver nanoparticless in an environmentally benign manner. One crucial, efficient, and innovative technique for producing silver nanoparticless is the green manufacturing of silver nanoparticless. Silver nanoparticless have been attranmission electron microscopypted to be produced in this study using the simple green approach. An interesting feature of this synthesis is the stabilisation of silver nanoparticless by ocimum tenuiflorum and associated plant extracts [2].

In this study, fresh juice and decoction of the plant ocimum tenuiflorum (thulasi, also known leaves) were used to create silver nanoparticles. Because of its chemical contents (oleanolicacid, ursolicacid, rosmaricacid, eugenol, methyl chloride, and caryophyllene), it has numerous uses in various sectors and is therefore considered a phytomedicine. Thulasi leaves are reported to have greater antioxidant capacity than thulasi stranmission electron microscopys, and ocimum tenuiflorum has a number of beneficial properties, including cardiac, antidiabetic, and anticancer effects. Additionally, it is employed to defluoridate water.

Previous studies have shown the enormous potential of the silver nanoparticles derived from thulasi extract. Silver nanoparticles' antibacterial effectiveness against bacteria like Staphylococcal aureus and E. Coli was further studied and utilised for specific applications since they are easily encapsulated by proteins and metabolites. These silver nanoparticles are useful as antimicrobial agents in the food [3], cosmetic, textile dye, and dressing sectors, as well as in medicine to treat vibriodisease and as a good genoprotectant. In this work, extract from the leaves of ocimum tenuiflorum (thulasi) was used to create silver nanoparticles under three distinct deposition conditions:

- At standard transmission electron microscopy temperature, combine the thulaside mixture with silver nitrate.
- Adding thulasi concoction to silver nitrate while stirring constantly at a high transmission electron microscopy temperature.
- Blending thulasi juice with silver nitrate solution for a long period of two hours.

Scanning electron microscopy, energy dispersive x-ray spectroscopy, transmission electron microscopy, hrtranmission electron microscopy, saed, and uv-vis were

used to characterise the silver nanoparticless in relation to variations in the deposition conditions. The findings are thoroughly examined.

2. METHODOLOGY OF SYNTHESIS

Using an extract from thulasi leaves as a reducing agent, silver nanoparticles (flower form) are synthesised at ambient transmission electron microscopy temperature and at elevated transmission electron microscopy temperatures.

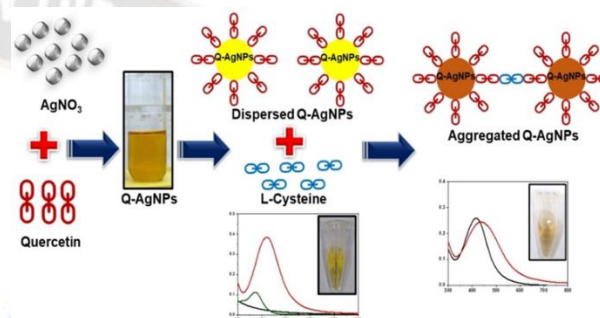


Figure 1: Synthesis of silver nanoflowers (AGNFS)

2.1 AGNP susing thulasi juices synthesis as a reducing agent

Silver nitrate and thulasi as a reducer were used to create silver nanoparticless.fresh thulasi leaves are gathered and thoroughly cleaned three times with distilled water to make the thulaside concoction.three grammes of leaves were added to 100 millilitres of water, which was then heated to a boiling point using a magnetic heater. After filtering, the pale green solution was used to produce ag nanoparticles.using a pestle and mortar [4], the leaves are pounded before being combined with the right amount of water to make green thulasi juice. A 100 ml solution of 1 mm silver nitrate was prepared.

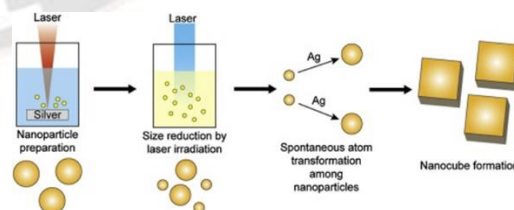


Figure 2: Synthesis of spherical silver nano particles

Three distinct synthesis methods and conditions were used to create silver nanoparticles. These included

raising the transmission electron microscopy temperature, adding pure darker-colored juice from the exact same plant leaves, and extending the time the solution containing silver nitrate was in solution. It was noted that the tint changed from white to reddish brown. The colour changes sharply in the high-stirred solution with thulasi juice among the three techniques mentioned above.

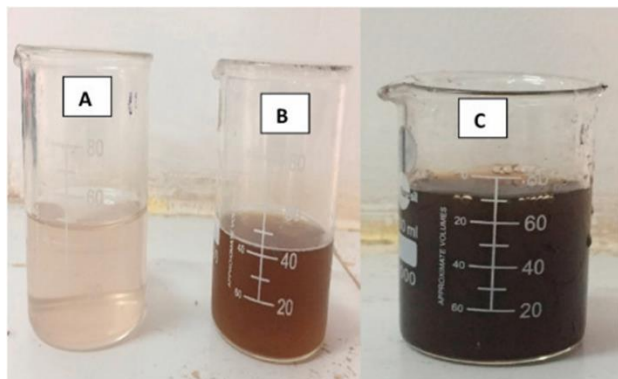


Figure 3: Images of silver nanoparticles using thulasi leaf extract under three conditions: (a) tn & tdn silver nanoparticles at standard and increased transmission electron microscopy temperature, (b) tr using thulasi juice

2.2 Characterization

The produced materials were characterized by energy dispersive x-ray spectroscopy peaks for chemical analysis, uv-v is spectrometry for absorption spectrum analysis, and microscopy for morphology and grain size [5].

3. Scanning electron microscopy analysis

The shape of silver nanoparticles was investigated, and the grain size of the three samples was estimated using scanning electron microscopy analysis. Silver nanoparticles with a flower-like form and high grain sizes of 90 to 170 nm are made at standard transmission electron microscopy temperature using a thulasi mixture. The grain size of silver nanoparticles produced (by thulasi decoction) at high transmission electron microscopy temperatures is less than 90 nm. However, the grain size of the silver nanoparticles recovered by thulasi juice is only about 50 nm. Due to the presence of raw phytochemicals, the synthesis method employing thulasi raw juice produces nanoparticles with a spherical form, which is distinct from the other two synthesis methods. Fig 4, 5, and 6 showed the

nanoparticles' form in relation to the deposition circumstances. Fig 4 shows the silver nanoparticles made from the decoction of thulasi plants extract at normal transmission electron microscopy temperature, fig 5 shows the silver nanoparticles made from the infusion of thulasi leaf extract at a high transmission electron microscopy temperature, and figure 6 shows the silver nanoparticles made utilising the juice of thulasi leaves as a reduction agent.

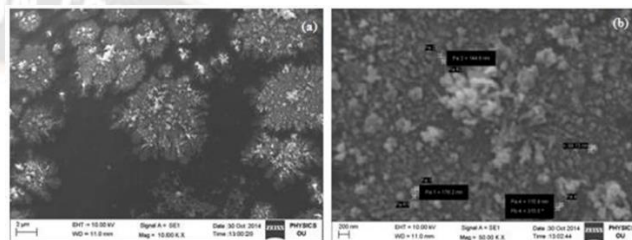


Figure 4: Scanning electron microscopy pictures of the grain size and morphology of silver nanoparticles produced at standard transmission electron microscopy

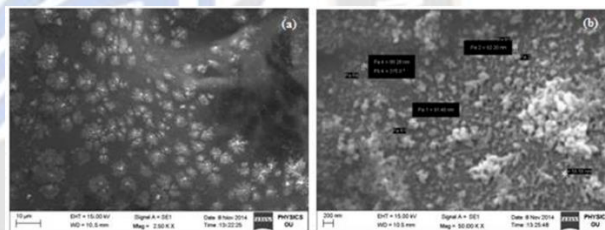


Fig 5: Scanning electron microscopy images of (a) morphology and (b) grain size of silver nanoparticles formed at 80°C transmission electron microscopy temperature from agno_3 solution

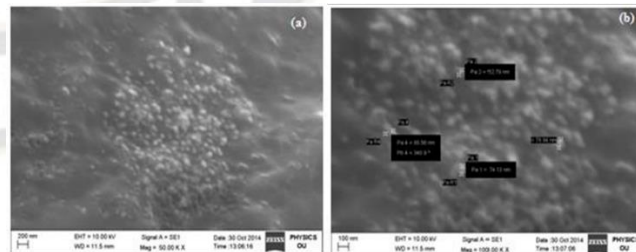


Fig 6: Scanning electron microscopy images of (a) morphology and (b) grain size of silver nanoparticles formed with increasing stirring time of agno_3 solution

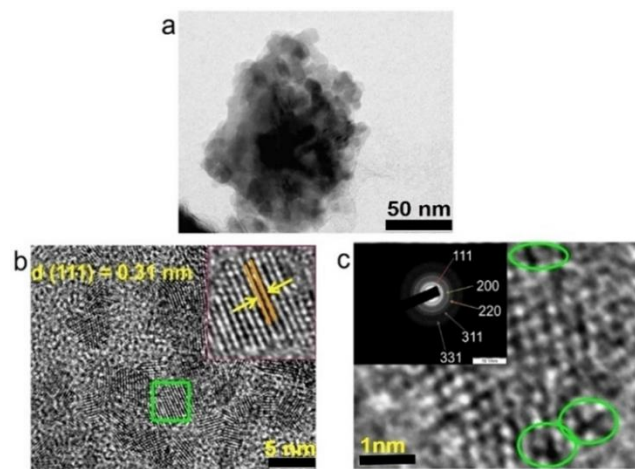


Figure 7: Structural characterization of silver nanoparticles at standard transmission electron microscopy temperature: (a) transmission electron microscopy, (b) hrtransmission electron microscopy, and (c) saed images

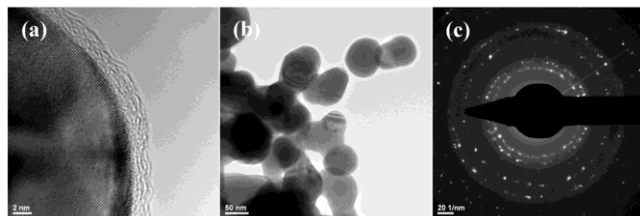


Fig 8: Structural analysis of silver nanoparticles at 80°C: (a) transmission electron microscopy, (b) hrtransmission electron microscopy, and (c) saed images

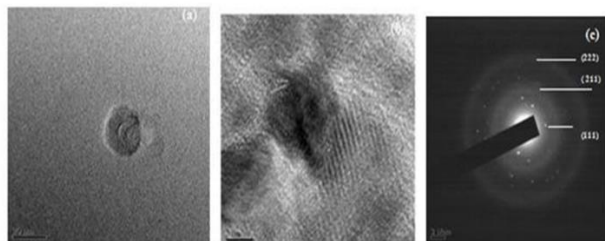


Figure 9: Structural characterization of silver nanoparticles after 2 hours of stirring: (a) transmission electron microscopy, (b) hrtransmission electron microscopy, (c) saed images

The saed, the use of hrtransmission electron microscopy, and transmission electron microscopy visualisations of silver nanoparticless produced at standard transmission electron microscopy temperature by thulasi decoction are shown in figure 7. The particles are round and have a mean size of about 50 nm. The diffraction pattern shows brilliant spots that are suggestive of a highly crystalline form, and the interplanar d-spacing is measured to be 0.25 nm. The (111), (200), (211), (311), and (222) planes' [6] associated diffraction rings are seen.

The transmission electron microscopy, hrtransmission electron microscopy, and saed images of silver nanoparticless produced by thulasi decoction at 80°C are displayed in fig 8. With an average size of 20 nm and a d-spacing of 0.23 nm between neighbouring surfaces, the particles have a flower-like appearance. For the (111), (200), (211), and (311) planes, diffraction rings are seen. The spherical silver nanoparticless made with thulasi juice had a d-spacing of 0.14 nm between adjacent planes and a particle size of 10 nm. Fig 9 displays the transmission electron microscopy, hrtransmission electron microscopy, and saed images of these silver nanoparticles, which were created using thulasi juice at standard transmission electron microscopy temperature and stirred for two hours. The pattern shows diffraction rings for the (111), (200), and (211) planes.

3.1 UV-visible spectroscopy analysis

The samples made with thulasi leaf decoction as a reduction factor at an ambient and elevated transmission electron microscopy temperature, respectively, showed the highest absorption peaks at 460 nm and 436 nm. figure 10 displays the study of the silver nanoparticles (a) using uv-visible spectroscopy. formed at standard transmission electron microscopy temperature and (b) formed using a thulaside mixture at a high transmission electron microscopy temperature of 80°C. Similarly, fig 11 displays the uv-visible spectroscopy study for silver nanoparticles made solely with thulasi juice [7], with the greatest absorption peak detected at 460 nm.

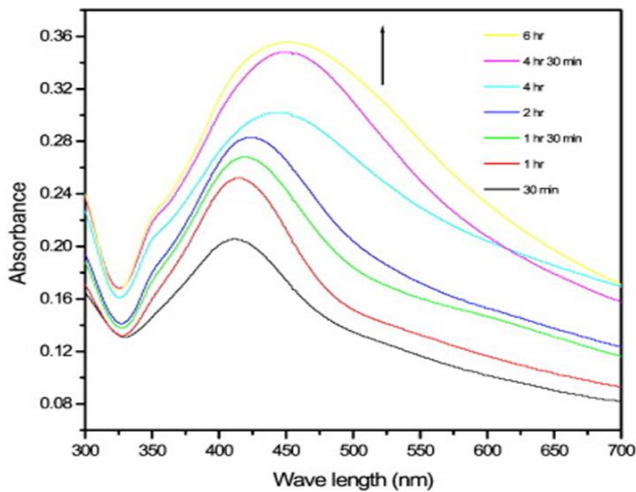


Figure 10: Ag nanoparticles uv-v is spectrum at ambient transmission electron microscopy temperature 80°c.

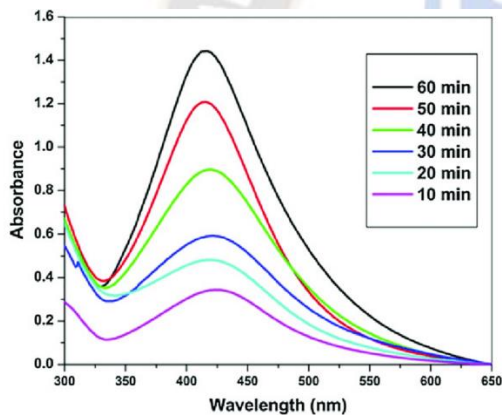


Figure 11: UV vis spectrum of silver nanoparticles using thulasi juice

3.2 Energy dispersive x-ray spectroscopy analysis

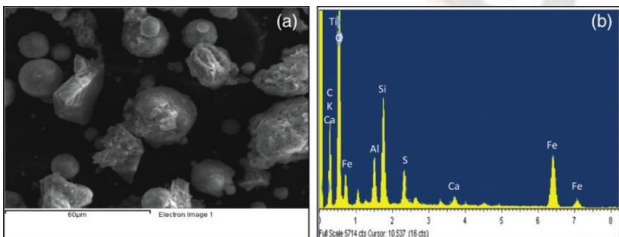


Fig 12: Energy dispersive x-ray spectroscopyspectrum of agnp sat (a) at standard transmission electron microscopy temperature (b)

at the 80°c transmission electron microscopy temperature

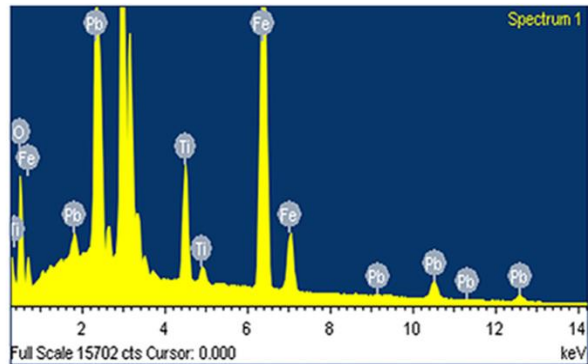


Figure 13: Energy dispersive x-ray spectroscopy spectrum of silver nanoparticles using fresh thulasi juice

Table 1: Elemental analysis of Ag (silver nanoparticles) using energy dispersive x-ray spectroscopy.

Metal	Percentage by weight	Percentage by atomic
Silver lattice	100	100
Overall	100	

Spectra from energy- dispersive x-ray spectroscopy offer an investigation of the silver nanoparticles composition. The production of pure tiny silver particles in this preparation was confirmed by the results of energy dispersive the x-ray spectroscopy spectra, which surprisingly showed no indications of contamination. Fig 13 illustrates how the juice of thulasileaves was used as a reduction agent to make silver nanoparticles, whereas Fig 12 (a) and (b) illustrate a combination of ocimum tenuiflorum leaf extract.

4. Outcome

Ocimum tenuiflorum (thulasi) leaf were used as a reduction agent in the synthesis of silver nanoparticless. Various synthesis methods led to variations in grain size and morphology, and table 2 shows that the absorption spectra also varied with synthesis method [8].

Table 2: Results of AGNP synthesis using thulasi leaves

S.no	Plant	Transmission electron microscopy temperature	Scanning electron microscopy analysis		Energy dispersiv e x-ray spectroscopy	Transmissi on electron microscopy Particle size (nm)
			Grain size (nm)	Form		
1	Thulasi decoction	Standard transmission electron microscopy temperature	90to170	Spherical	Silver	50
2	Thulasi decoction	80°C	Less than90	Flower	Silver	20
3	Thulasi juice	Standard transmission electron microscopy temperature	50	Spherical	Silver	10

The significant therapeutic value of *Ocimum tenuiflorum* leaf makes these silver nanoparticles suitable for usage in the pharmaceutical industry. Stabilised particles and their pharmacological uses are the subject of ongoing research.

5. Integration of Silver nanodendrites: One-step green synthesis produces silver nanodendrites that develop spontaneously with nanostars and several branches similar to nanoneedles.



Figure 14: Snowflake dendrite form

The theoretical explanation of dendritic form is not a novel idea. Before the existence of atoms was acknowledged, Kepler investigated the dendritic form of snowflakes, as seen in figure 14. Metals undergo vapour phase, liquid phase, and solidification to generate dendritic formations. Rapid growing grains with a high surface-area-

to-volume ratio will be produced by thermal procedures, resulting in dendritic growths that resemble scanning electron microscopy (SEM) images of spiky fir trees. Numerous mathematical and theoretical formulas have been created to address dendritic issues [9].

Metal dendrites are used in many different fields. Copper dendrites are beneficial for microdevices and electrode changes. The effectiveness of Pd-Cu bimetallic nanodendrites as a catalyst for oxygen reduction reactions has been demonstrated. Electronic and photonic systems using transmission electron microscopy frequently use magnetic fractal forms, and fractal shapes of magnetism nanoformed materials are a crucial component of nanotechnology. Nanomaterials are utilised in batteries and sensors. Au nanodendrites had a special activity of electrocatalytic reduction of H_2O_2 and showed more sensitivity detection.

Silver nanodendrites, among other metal dendrites, have garnered interest because of their numerous uses in the sectors of business and health. Human T-lymphotropic virus type-I (HTLV-I) DNA can be detected by silver dendrites in the medical field, and chitosan-conjugated dendrites are used to kill malignant cells by photothermal means. Dendritic silver nanoforms have excellent catalytic activity and are utilised to reduce p-nitrophenol. It is also useful for the electrocatalytic oxidation of both formaldehyde and hydrazine as well as oxygen reduction. The conductive filler for electrically conductive adhesives is silver nano and

nanodendrites. These nanodendrites demonstrated a high degree of humidity sensing capabilities [10-12].

Ag nanodendrites, or agnds, are used extensively due to their effective improved qualities. These are the best catalysts, according to a prior agnds evaluation, because of their high crystalline nanoparticles and huge surface space to volume ratio. Agnds with excellent properties such surface enhanced fluorescence, super hydrophobic surface, and surface enhanced Raman spectroscopy is useful for chemical investigation of materials and sensitive interfacial research [292]. Luminescent silver nanodendrites guided by cholic acid (ca) biomimetic synthesis are a powerful inhibitor of hiv-integrase. Agnds are used in biosensors and biomedicine [293]. For crucial optoelectronic applications, such optical interconnectors and displays, electroluminescence of out-of-plane silicon nanotube/silver oxide/silver nanodendrite hetero form devices eliminates the need for costly direct band gap materials.

Numerous chemical, physical, and biological techniques are available to prepare silver nanodendrites, including solvothermal, liquid phase reduction, hydrothermal manufacturing, deposition of chemical vapour, photolithography-assisted wafer measure fabrication, electrochemical methods electrodeposition, metallic electromigration, galvanic stimulation displacement procedure, and ultra violet photoreduction technique.

However, the green synthesis procedure is the most affordable and user-friendly approach when compared to the physical, chemical, and electrical approaches previously discussed. According to reports from K. Piper betel leaf extract was used to create silver nanoparticles (silver nanoparticles). However, this is nearly the first transmission electron microscopy to use piper betel leaf extract to create silver nanodendrites (agnds). Without the use of harsh chemicals, electric fields, additives, transmission electron microscopy plates, high transmission electron microscopy temperatures, metal substrates, or surfactants, silver nanodendrites were created utilising the green technique [13].

Piper betel leaf broth was used as a reducing agent to create silver nanodendrites for the current study. In India, especially in southern India, the leaves of the piper betel plant are eaten orally (with nut powder, tinge, or hint of calcium carbonate), and they are often eaten after meals. It belongs to the piperaceae family. Antioxidant, antifungal,

antibacterial, and anti-inflammatory properties are just a few of the many medical benefits of betel leaves. Betel leaves function as an antidiabetic and bioprotective agent. Additionally, rheumatism, stomach aches, bronchial asthma, wind-cold, cough, and pregnant oedema are all treated with it. Excessive bleeding during menstruation can be stopped with it. The leaves have stimulating properties. This extract can lessen stomach pain and nausea. Betel leaves are used for cardiovascular, fatigue, and fever. Hepatoprotective, neuroprotective, anti-ulcer, and immunomodulatory effects of leaves are revealed by research on them. Research on the leaves of betel trees has shown that they are not only an excellent mouth freshener but also an effective antidepressant, and they also lessen halitosis. These leaves can heal wounds, and their antiviral properties have shown promising results against streptococcus mutans.

The development and spread of plaque-producing bacteria are inhibited by these leaves. The finest stimulator of pancreatic lipase and digestion are betel leaves. Microscopy of a longitudinal section of leaves shows that the mesophyll tissue system transmission electron microscopy contains a variety of cell shapes. Dendritic form is determined by the tissue system transmission electron microscopy's mesophyll.

Scanning electron microscopy, transmission electron microscopy, saed, uv-vis spectroscopy, and energy dispersive x-ray spectroscopy were used to characterise the produced silver nanodendrites.

5.1 Synthesis

First, a 1 mm silver nitrate solution was made with double-distilled water to create silver nanodendrites. Fresh piper betel nut leaves were cleaned three times and removed with a cotton cloth in order to prepare the extract. The leaves were cut finely and let to air dry. After that, the leaves were cooked for 20 minutes in 50 millilitres of purified water. The resulting solution had a light yellow hue. This leaf extract was added to a 1 mm silver nitrate solution that had been made at 450 degrees Celsius beforehand. The solution was pale at the start of the reaction before turning white. A change in hue over time signifies the formation of silver nanodendrites in the solution.

In the condition of piper betel leaf in the broth, the liquid silver nitrate was first converted to silver nanoparticles. Then, the silver particles grew in the solution,

forming dendrites as seen in figures 15 and 16. Heat is produced at the moment of reaction. The transmission electron microscopy temperature of the entire solution rose when silver dendrites began to grow in the leaf broth solution. This transmission electron microscopy temperature is higher than the initial leaf broth and silver nitrate solution. This transmission electron microscopy temperature dropped in a matter of seconds. It appears that this reaction is exothermic.

Scanning electron microscopy, transmission electron microscopy, energy dispersive x-ray spectroscopy, saed, and uv-vis were used to characterise the produced silver nanodendrites.

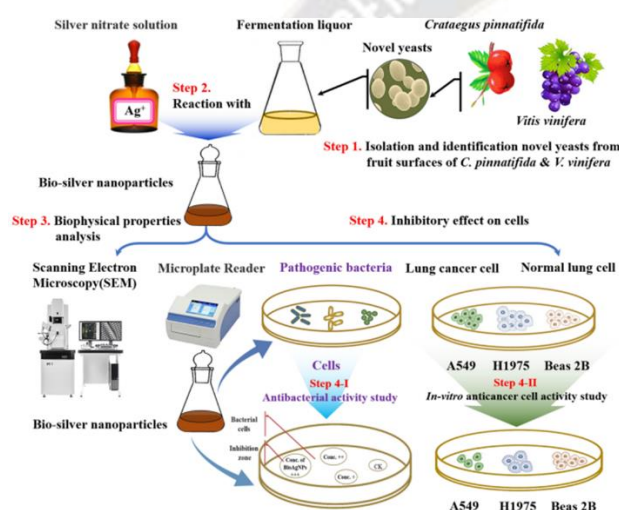


Figure 15: Synthesis of silver nanodendrites and nanostars using piper betel leaf broth

5.2 Betelleafbroth

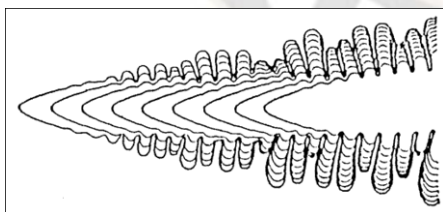


Figure 16: Dendrite growth from melt

5.3 Characterization: Scanning electron microscopy

The silver nanodendrite (tree)like form was demonstrated and validated by the scanning electron

microscopy micrographs seen in figures 17 and 18. Silver nanostellars as well as silver nanodendrites are confirmed in the scanning electron microscopy image.

Multiple branches were grown on silver nanodendrites. In a scanning electron microscopy image, broken branches are clearly visible. These branches have recollected original branches that are 1–3 μm long and have spike or needle-like crystals. Secondary nanobranches, ranging in size from 80 to 500 nm, are growing on these main branches. The growth only ceased with secondary branches because there was not enough space between the dendrites. Tertiary limbs were also cultivated for dendrites that had more standard surrounding secondary branches.

These secondary branches rescanning electron microscopy the form of a pine tree. nanoneedles between 200 and 300 nm in length were seen in these formations.

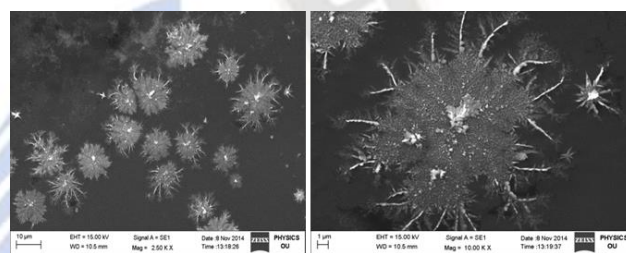


Figure 17: Scanning electron microscopy image of ag nanodendrites (AGNDS) at different magnifications



Figure 18: Scanning electron microscopy image of silver nanodendrites and nanostars

5.4 Transmission electron microscopy

In figure 19, transmission electron microscopy images of silver anodendrites were displayed. It is evident that ag has a drete (tree-like) form. broken branches with a sharp tip and a length of 50 nm were visible in the transmission electron microscopy picture. Spherical silver

nanoparticles are attached to produce these branches of silver nanodendrites, which have extremely sharp tips and a triangle-shaped particle at the needle's edge. Transmission electron microscopy images show the form connection between the particles in the knee joint. The length of the major and secondary branches is 20 nm.

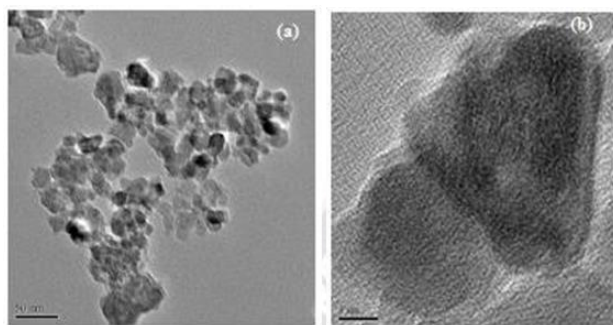


Figure 19: (a) Transmission electron microscopy image of ag nanodendrites (agnds) and (b) tip of the nanoneedle of agnds

5.5 Saed:

The saed of agnds is shown in figure 20. The brilliant spots of the diffraction pattern were seen in the picture. These brilliant spots suggest that the dendrites are single crystalline, and the planes (111), (200), (220), (311), (400), (420), and (422), as well as the diffraction pattern, are visible.

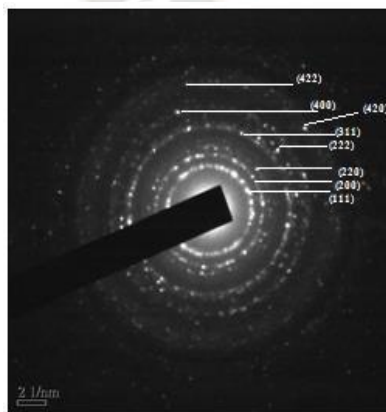


Fig 20: Saed pattern of silver nanodendrites

5.6 Energy dispersive x-ray spectroscopy:

Table 3: Elemental analysis of silver nanodendrites

Element	Percentage by weight	Percentage by atomic%
Silver lattice	100	100
Overall	100	

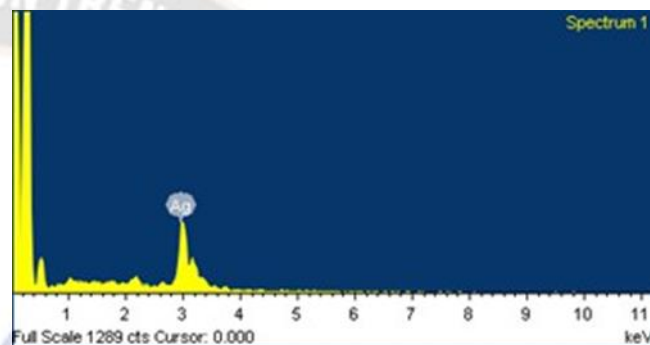


Figure 21: Energy dispersive x-ray spectroscopy analysis of silver nanodendrites

Fig 21 displays the single peak from the sample in the energy dispersive x-ray spectroscopy spectrum. The sharp straight peak in the energy dispersive x-ray spectroscopy analysis indicates that there is only one silver element in the sample. The presence of only pure silver created in this synthesis technique was revealed by the single silver peak, which also demonstrates that no other contaminants were generated throughout the preparation procedure.

The elemental examination table 3, which shows that 100% silver was present in the final product, is supported by the energy dispersive x-ray spectroscopy analysis. Therefore, energy dispersive x-ray spectroscopy analysis is the appropriate technique to obtain purified silver nanodendrites (agnds).

5.7 UV visible spectroscopy

Silver nanodendrites' uv-vis spectroscopy is displayed in figure 22 below. Silver nanodendrites' highest absorption spectra were detected at 436 nm. The wavelength

of the absorption peak is in the category of visible light, as indicated by the greatest peak of the uv-visible spectrum.

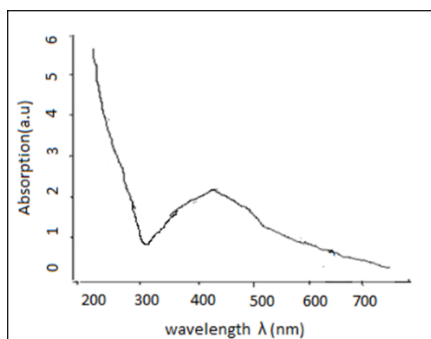


Figure 22: Uv-vis spectroscopy of ag nanodots

5.8 Outcome

There are many uses for silver dendrites in the production of sensors. The shape of silver nanoparticles determines their characteristics. A variety of transmission electron microscopy plates, surfactants, and reducing agents can be used to create different forms. In this study, piper betel leaves extract was used as a reducing agent in a single-step green synthesis to create silver nanodendrites without the need of any surfactants. Primary, secondary, and tertiary branches were generated in silver nanodendrites. A small number of dendrites feature needle-like crystals and a stellar form. Scanning electron microscopy characterisation verified the development of silver nanodendrites, transmission electron microscopy determined the particle size, and energy dispersive x-ray spectroscopy examined the purity of the silver nanodendrites. Spectra of absorption were found in the visible range of 300–700 nm.

This study shows the ability of a strong piperbetelle extract in addition to presenting a novel technique for the production of silver nanodendrites utilising an easy, green method. Silver nanodendrites can be made with a piperbetelleaf and a straightforward green technique. This procedure also creates silver nanodendrites with all three types of branches, as well as nanostars.

6. Synthesis of silver nanorods by single replacement reaction

Nps in a variety of shapes, including rods, wires, flowers, and dendritic forms, have been successfully

synthesised and have been shown to have unique behaviours that rely on other topological factors in addition to size. Nanorods are one-dimensional nanomaterials that are artificial and do not occur in nature. These nanorods were produced by direct chemical synthesis, which is the procedure of conducting chemical reactions with a specific end result in mind. Metal-organic chemical vapour deposition, electrochemical reduction, seed-mediated surfactant, transmission electron microscopy plate, vapour phase, and hydrothermal reaction are methods that can be used to create nanorods made from gold (gnrs) and zinc oxide nanorods (zno nrs).

A specific combination of ligands, surfactants, and reducing agents gives the nanorod its elongated rod shape by binding to different regions of it with differing strengths, which enables them to grow at varied rates. A method for creating long silver nanorods by adjusting the growth solution's volume is described. We saw shapes ranging from 1d rods to fusiform (broad in the middle and tapered at both ends) nanoparticles. The length of those nanorods can be controlled by increasing the growing solution. Because of their special qualities and uses, nanorods are inspiring researchers. After being created, nanorods can be used in a variety of ways.

Zno nanorod bio sensors are a promising option for highly sensitive electrical detection of biological species, and due to the fact that nrs have been shown to lower the bacteria *E. Coli*, zno can also be utilised as a water disinfectant. Gold nanorods (gnrs) have been employed as color-polarizing filters with success. The malignant tissues have been successfully eradicated by gnrs. Using two-photon luminescence (tpl) microscopy, *Bacillus subtilis* spores—a simulant of *Bacillus anthracis*—have been imaged using gold nanorods (gnrs). Their NIR absorbance property has allowed for improved picture contrast in photoacoustic scanning.

Many techniques have been investigated in the survey to create silver nanorods (ag nrs). These include transmission electron microscopy temperature-dependent procedures, wet chemical reduction, UV irradiation photoreduction techniques, microwave synthesis techniques, and electrochemical and sonic electrochemical methods.

Because of their surface plasmon effects, silver nanorods have a high sensitivity and may identify respiratory viruses rapidly effective inks with conductivity can be produced as a final product by using silver nanorods. Silver nanorods (agnrs) are able to identify the presence of bpo (benzoyl peroxide), a colourant that is detrimental to food itransmission electron microscopys. Silver nanorods are valuable in play technologies because an electric field can modify their reflectivity, which in turn alters their orientation.agnrs are used in a number of applications, including electrical, photocathode, plasmonic, and antimicrobial ones. Because of its superior optical qualities in the blue wavelengths, agnrs are successfully used in phosphorescent blue organic energy dispersive x-ray spectroscopy as well as in spasers (nanoscale lasers).

Mercury ion detection is a good use for ag nrs produced by galvanic replacements reaction. Nanorods are also used in cancer treatment. Micro electro mechanically systransmission electron microscopy and nano electrochemical mechanical engineering devices (mems and nems), as well as bio-nanomaterials like biomarkers, biondiagnostics, and biosensors, and related nanomaterials, can benefit from the use of silver nanorods in nano electronics and photonics. These are useful in polymers, textiles, food, fuel cell layers, composites, and solar energy materials. They are also utilised in photothermal therapy, surface enhanced spectroscopies, and plasmonic regulators. Escherichia coli bacteria are susceptible to the antibacterial properties of these silver nanorods.

The synthesis of silver nanorods is easier and less expensive than that of other nanorods. It primarily involves the reduction and transmission electron microscopyplate procedures, which may be utilised to make silver nanorods and silver nanorod arrays.

Silver nanorods can be created using a synthesis that doesn't require a transmission electron microscopyplate, seed, or surfactant. This paper presents the investigation of the reduction procedure, and the method's description offers flexibility to repair various nanorods.the challenge is to create silver nanorods without the use of surfactants, transmission electron microscopyplates, or seenenergy dispersive x-ray spectroscopy.one example of it is silver nanorods made using the reduction procedure. Ag nrs made

with tri-sodium citrate as a reduction agent have already been described by the jian-qiang hu team. Groundwork reduction requires less money and energy, and this approach is nontoxic and environmentally benign. Large amounts of silver nanorods were obtained in this synthesis, according to scanning electron microscopy and transmission electron microscopy images. To create ag nrs, we have chosen the standard reduction approach, which requires minimal equipment and only requires one chemical—silver nitrate solution and copper rod—making it a simple one-step procedure for the nanorods. High-crystalline silver nanorods are produced by the reduction synthesis, which is compared to earlier strong-reducing agent syntheses.

6.1 Synthesis: Single replacement reaction

In a silver nitrate solution, copper metal is dissolved.the reaction's balanced equation is as follows:

$$\text{Cu(s)} + 2\text{silver nitrate(aq)} \rightarrow 2\text{(aq)} + 2\text{ag(s)} + \text{cu(no3)}.$$

- Oxidation half-reaction 2e^- -(oxidation) + $\text{cu} \rightarrow \text{cu}^{2+}$ -
reduction half-reaction
- $3\text{ag} \rightarrow 2\text{e}^-$ (reduction) net reaction: $\text{cu(no3)} + 2\text{agCu} + 2\text{silver nitrate} = 2$

In order to decrease silver (ag), two electrons must be acquired, while copper (cu) is oxidised by losing two electrons. Copper is a reducing agent and silver is an oxidising agent.

We concentrated on silver (ag) in this study because of its many uses and adaptable qualities, which give it a higher potential value (+0.800v). Since silver is a stable metal and its ions may be readily reduced to other metals, it lies at bottom of the series. The inclination to reduce will increase with a higher reduction potential value. Relative replacement propensity is shown by this possibility.ag will be removed from the silver nitrate solution by cu.

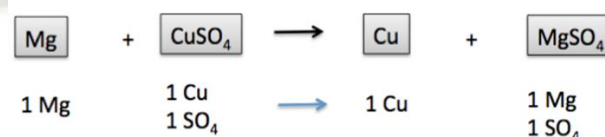


Figure 23: Procedure of a single replacement reaction

To examine the outcomes of a single replacement reaction between a copper rod and a silver nitrate solution, we use transmission electron microscopy in this work. We watch the process as the silver solution with nitrates transforms into nanorod-shaped silver particles.

The morphologies of the silver nanorods and those observed in ex situ testing for control are fairly similar. The rates of reaction, however, are far higher. Given its greater reactivity than silver, copper takes the place of silver in this process. Copper is more stable in this process because of its reduction potential. This explains why more stable nanoparticles of silver were obtained using this procedure.

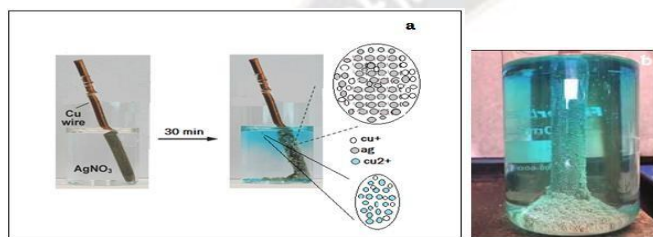


Figure 24: (a) single displacement reaction and (b) accumulation of silver nanoparticles after one day

It was noted that the solution turned blue and a solid with a dark ash colour formed in the bottom of the glass beaker. The development of silvery silver nanoparticles gathered at the bottom is shown by the solid ash colour. Cu^{2+} ions are indicated by the blue solution, while Cu^{+} ions are indicated by the small amount of white solution.

6.2 Development of silver nanorods

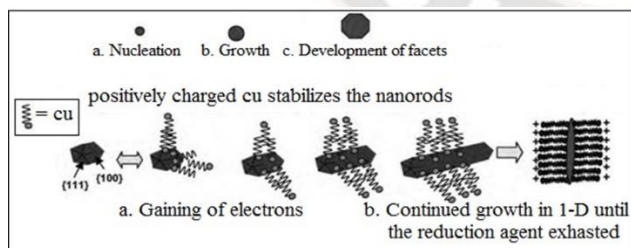


Figure 25: Growth mechanism of silver nanorods

The reaction solution was initially white in hue. The silver nitrate solution's hue turned blue with time, and silver began to collect at the bottom. Agnr growth is depicted

in figure 25. As seen in figure 25 (a), silver gained electrons from copper to lengthen its form. Figure 25 (b) and (c) illustrate how the copper has an effect on the silver atoms that receive electrons, which causes the manipulated region to expand in a particular direction. It's a lengthy procedure because the original solution were half blue and half white, but after a day, the whole thing changed blue. Silver small rods will form until all copper's electrons run out. This entire blue colour means that platinum is growing fully while copper is running low. Silver particles produced by this procedure are more stable since silver has a low oxidation potentially they collected the particles.

6.3 Characterization

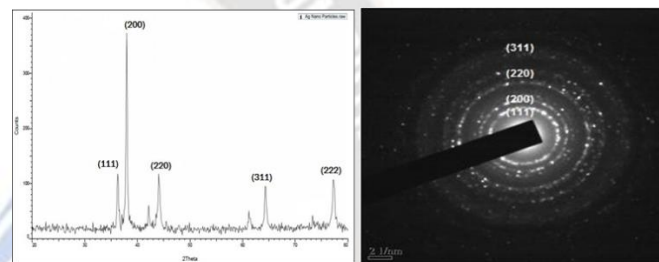


Figure 26: Silver nanorod XRD pattern Figure 27: Silver nanorods in a saed pattern

Material's acrySTALLINE nature and fcc crystal form are demonstrated by the xrd sharp peaks in figure 26. Peaks have been credited to the refraction from sectors of (111), (200), (220), (311), and (222) of silver nanorods, per (jcpdsno:04-0783).the mean crystal size of the angorods produced during the reduction procedure was measured using debye-scherrer's formula. The pristine state of the sample is indicated by an appearance of impurities peaks in the xrd peaks.based on the (111) preferred orientation, the crystallite size for ag nrs synthesised during the reduction procedure was found to be 20 nm.

The saed image of the diffraction pattern's bright regions is displayed in figure 27.The diffraction pattern indicates that the bright spots in planes (111), (200), (220), and (311), reveal that the silver nanorods are single-cryline in character. The four important circular forms (111), (200), (220), and (311) that are confirmed by xrd data and correspond to the distinct peaks of the cubic with a face crystal arrangement are seen in figure 27. The chosen area diffract electron (saed analysis) pattern of anorods is as

follows. the growth direction typically follows the basic fcc ag-form's (111) zone axis.

The polished diameter of the silver nanorods and their favourite orientation of crystals along the 111, 200, or 220 crystalline planes are briefly examined [346,347,348,349,350].

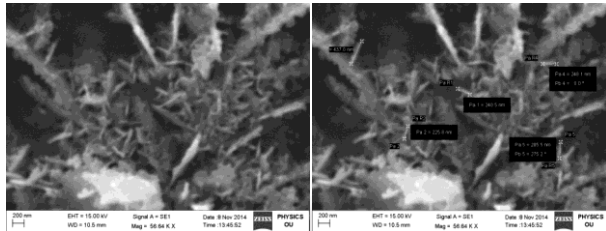


Fig 28: (a) scanning electron microscopy image of silver nanorods (agnrs) and (b) grain size distribution of silver nanorod

The photos from scanning electron microscopy demonstrate the unique shape of the silver nanorods, which are 20–200 nm long. Thenanorods are typically 20 nm long. According to the scanning electron microscopy analysis, this is the most effective strategy for producing silver nanorods in large quantities.

The majority of the products made using the soft transmission electron microscopy plate method are uniform ag nanorods with a diameter of 40 nm and a length of 140 nm, according to scanning electron microscopy images displayed in figure 28 (a) and (b) nevertheless, there are nanocrystals with different forms and some nanorods that are much larger than this range. A few nanorods are about 200 nm, according to scanning electron microscopy. The reason for this is that the micelle transmission electron microscopyplate hypothesis, which states that a micelle is an asscanning electron microscopyblage of surfactant molecules scattered in a liquid colloidal, can be used to explain this occurrence. Some of the seenenergy dispersive x-ray spectroscopy are in the micelle controlled region when they are added to the reaction solution, while others are outside of it. Only along the longitudinal direction may ag seenenergy dispersive x-ray spectroscopy grow in a micelle-controllable zone, producing homogeneous, controllably sized nanorods.conversely, the growth of ag seenenergy dispersive x-ray spectroscopy outside of the microelle-controllable zone is unrestricted in many ways,

resulting in the production of enormous nanorods and various forms.

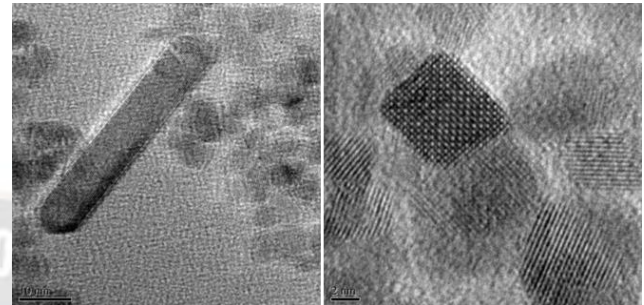


Figure 29: (a) transmission electron microscopy image and (b) hrtransmission electron microscopy image of ag nanorods

Transmission electron microscopy images produced by the reduction procedure of the material extracted from the bottom of the beaker.transmission electron microscopy pictures showed the formation of empty silver nanorods that were 10 nm in size.the ag nanorods' crystallinity is further confirmed by the high-resolution images transmission electron microscopy (hrtransmission electron microscopy) in fig 4(c) above fig 29 (a) 7(b) the nanorods are single-crystalline they expand in the (111) [14] direction, as indicated by their spacing between lattices of 0.236 nm.

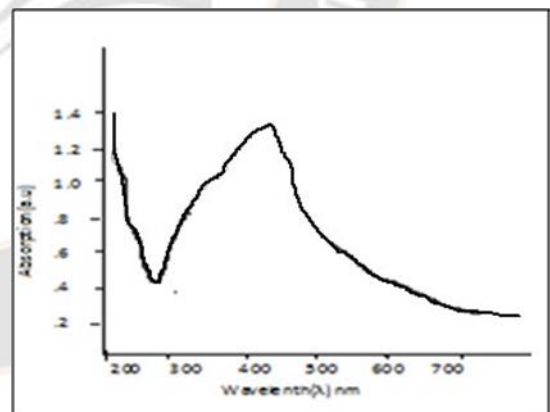


Figure 30: Ultraviolet-visible-vis spectroscopy analysis of ag nanorods (agnrs)

Agnrs' uv-visspectroscopy is displayed in figure 30 .the optical absorption spectra of the majority of silver nanorods and nanowires show peaks at wavelengths between 350 and 450 nm.the optical absorption spectra of

these silver nanorods [15] shows maxima between 400 and 500 nm. By varying the size of nanorods, the long-range plasmon mode may be tuned over a broad spectrum, including the visible and in the near-infrared areas.

7. Conclusion

A simple technique for producing silver nanorods (ag-nrs) with only one substitution reaction is demonstrated in the current work. This agnr synthesis method is simple to make, low-cost, and involves no dangerous ingredients—all it needs are extracted beakers. With this method, large-scale ag-nrs can be obtained. A scan of the scanning electron microscope image revealed that most of the silver tiny rods were 20 nm, although a few were 200 nm. Images obtained by transmission electron microscopy reveal that these nanorods are 10 nm in size. The four prominent circular fringes indicated by the saed pattern (111), (200), (220), and (311), correspond to the characteristic peaks of the face-centered cubic crystalline structure. There are peaks in the 400–500 nm range of the silver nanorods' optical absorption spectrum.

References

- [1] Baruah, Kakali, et al. "Ocimum sanctum mediated green synthesis of silver nanoparticles: A biophysical study towards lysozyme binding and anti-bacterial activity." *Journal of Molecular Liquids* 337 (2021): 116422.
- [2] Priyadarshini, S., Sulava, S., Bhol, R. and Jena, S., 2019. Green synthesis of silver nanoparticles using *Azadirachta indica* and *Ocimum sanctum* leaf extract. *Current Science*, 117(8), pp.1300-1307.
- [3] Bindhani BK, Panigrahi AK. Biosynthesis and characterization of silver nanoparticles (SNPs) by using leaf extracts of *Ocimum Sanctum* L (Tulsi) and study of its antibacterial activities. *J. Nanomed. Nanotechnol.* S. 2015;6(008).
- [4] Jha, P.K., Jha, R.K., Rout, D., Gnanasekar, S., Rana, S.V. and Hossain, M., 2017. Potential targetability of multi-walled carbon nanotube loaded with silver nanoparticles photosynthesized from *Ocimum tenuiflorum* (tulsi extract) in fertility diagnosis. *Journal of Drug Targeting*, 25(7), pp.616-625.
- [5] Ahmad, M. Z., Alasiri, A. S., Ahmad, J., Alqahtani, A. A., Abdullah, M. M., Abdel-Wahab, B. A., ... & Alzahrani, S. A. (2022). Green synthesis of titanium dioxide nanoparticles using *Ocimum sanctum* leaf extract: In vitro characterization and its healing efficacy in diabetic wounds. *Molecules*, 27(22), 7712.
- [6] Mandal, A.K., Poudel, M., Neupane, N.P. and Verma, A., 2022. Phytochemistry, pharmacology, and applications of *Ocimum sanctum* (Tulsi). In *Edible Plants in Health and Diseases: Volume II: Phytochemical and Pharmacological Properties* (pp. 135-174). Singapore: Springer Singapore.
- [7] Melkamu Z, Jeyaramraja PR, Paulos T. Optimization of the synthesis of silver nanoparticles using the leaf extract of *Ocimum sanctum* and evaluation of their antioxidant potential.
- [8] Vijaya, P. P., B. Rekha, Anu Thersa Mathew, M. Syed Ali, N. Yogananth, V. Anuradha, and P. Kalitha Parveen. "Antigenotoxic effect of green-synthesised silver nanoparticles from *Ocimum sanctum* leaf extract against cyclophosphamide induced genotoxicity in human lymphocytes—in vitro." *Applied Nanoscience* 4, no. 4 (2014): 415-420.
- [9] Subbiah, R., Muthukumaran, S. and Raja, V., 2020. Biosynthesis, structural, photoluminescence and photocatalytic performance of Mn/Mg dual doped ZnO nanostructures using *Ocimum tenuiflorum* leaf extract. *Optik*, 208, p.164556.
- [10] Anandalakshmi, K., Venugobal, J. and Ramasamy, V.J.A.N., 2016. Characterization of silver nanoparticles by green synthesis method using *Petalium murex* leaf extract and their antibacterial activity. *Applied nanoscience*, 6, pp.399-408.
- [11] Singh, J., Singh, N., Rathi, A., Kukkar, D. and Rawat, M., 2017. Facile approach to synthesize and characterization of silver nanoparticles by using mulberry leaves extract in aqueous medium and its application in antimicrobial activity.